Proc. Natl. Acad. Sci. USA
Vol. 91, pp. 2930–2934, April 1994
Biophysics

Hydrodynamic steering effects in protein association

(cleft enzyme)

DOUGLAS BRUNE AND SANGTAE KIM*

Department of Chemical Engineering, University of Wisconsin, Madison, WI 53705

Communicated by R. Byron Bird, November 4, 1993 (received for review April 17, 1993)

ABSTRACT **Protein–ligand reaction rates are often limited by the rate of diffusional encounter of the protein and ligand in solution. Reaction rates, however, can be much greater than expected, given the necessity for correct orientation before reaction. A number of forces can affect the orientation of the protein and ligand in solution, and thus increase the reaction rate. We have considered hydrodynamic forces, produced when water molecules between protein and ligand must be pushed out of the way to allow their encounter. We have used the cleft enzymes as a model system, as they could be expected to show strong hydrodynamic effects. One particular type of hydrodynamic interaction stands out: a steering torque which occurs when the enzyme and substrate move toward each other in solution. The magnitude of this steering torque is compared to the mutual torque experienced by interacting "protein-sized" dipoles in solution. A simple model is used to demonstrate that the hydrodynamic steering torque can be 2 orders of magnitude greater than the electrostatic torque.**

The function of proteins almost inescapably depends on their physical interaction with other molecules, generally called ligands. Important examples of protein–ligand interactions include enzyme–substrate reactions; protein–nucleic acid interactions, when controlling replication and expression; and protein–lipid interactions during incorporation into membranes. In the words of Creighton (1), "Every aspect of the structure, growth, and replication of an organism is dependent upon such interactions."

Many protein–ligand reactions proceed with diffusion-controlled kinetics—that is, the rate-limiting step in the reaction is the diffusive encounter of the protein and ligand. The rate of diffusive encounter, k_D, can be estimated from the translational diffusion coefficients of the protein and ligand in solution, D_P and D_L, by treating the molecules as spheres that must approach within a distance r_{PL} to react:

$$k_D = 4\pi N_A (D_P + D_L) r_{PL},$$

or, when there is a net attraction or repulsion between the protein and ligand:

$$k_D = \frac{4\pi N_A (D_P + D_L)}{\int_{r_{PL}}^{\infty} \frac{\exp U(r)/kT}{r^2}\, dr},$$

where the interaction potential energy is given by $U(r)$, k is Boltzmann's constant, T is absolute temperature, and N_A is Avogadro's number. The diffusion coefficients can be measured experimentally or obtained from hydrodynamic mobilities. For an overview of this and other aspects of hydrodynamics in biophysics, see ref. 2.

The publication costs of this article were defrayed in part by page charge payment. This article must therefore be hereby marked "*advertisement*" in accordance with 18 U.S.C. §1734 solely to indicate this fact.

It is somewhat surprising that these equations predict reaction rates so well, because for many protein–ligand interactions, the molecules not only must be brought into close proximity but also must be oriented correctly in space for a successful encounter to occur. If these equations were to be corrected to allow reactions of correctly oriented molecules only (based simply on the fraction of solid angle available for reaction), they would predict association rates as much as three orders of magnitude too low (1). A modest increase can be obtained by considering the statistical likelihood of repeated encounters at different orientations (3), but this still gives a low estimate for the reaction rate. Clearly, there are some processes which act to orient the molecules prior to reaction, so that the orientation "penalty term" is not so severe.

There have been a number of explanations for the orientation that occurs prior to enzyme–ligand reaction. Prominent among these has been an explanation that involves electrostatic interactions. As a simple example, one could consider the steering torque produced by interacting electric dipoles. The dipoles act to orient the protein and the ligand, even as collisions from the thermal motion of surrounding water molecules bring the two close enough to react.

In addition to electrostatic forces, shorter-range forces such as van der Waals forces have been considered. In ref. 4, it is postulated that an attractive van der Waals force holds the ligand close to the protein until the ligand finds the orientation that allows a reaction.

There is another possible long-range force that can act to orient proteins and ligands in solution, namely the force that is produced by hydrodynamic interactions between the protein and ligand. It is common knowledge that many protein–ligand pairs exhibit complementary shapes (the so-called "lock-and-key" paradigm). If random thermal fluctuations push a protein–ligand pair together, the pair will be more favorably oriented for reaction by hydrodynamic interactions between the complementary shapes. Conversely, if thermal fluctuations drive a protein–ligand pair apart, the pair will be further disoriented by hydrodynamic interactions. This behavior, better orientation upon closer approach, is exactly what one would desire to increase the rate of reaction.

As an example, consider Fig. 1. The two bodies in this figure can be thought of as a cleft enzyme and a capsule-shaped substrate. To react, the substrate must fit into the cleft of the enzyme. As random thermal fluctuations drive the substrate and enzyme together, any skew between the axis of the enzyme cleft and the axis of the substrate will be corrected. An increased hydrodynamic force from the areas of the cleft that are closest to the substrate will cause the substrate to rotate, bringing the substrate and cleft into better alignment.

It is our aim to show that the magnitude of the hydrodynamic steering torque is in some cases at least as important as the electrostatic steering torque. We will compute the hydrodynamic steering torque in a mathematically rigorous

*To whom reprint requests should be addressed.

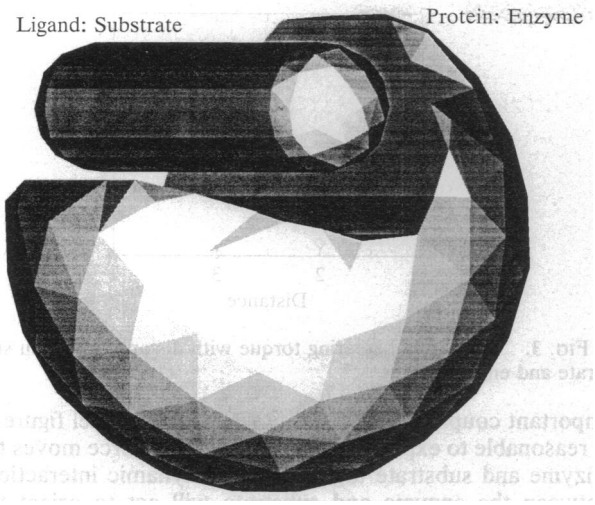

FIG. 1. Discretized representation of an enzyme–substrate reaction.

fashion (to the extent allowed by our continuum approach and simple model) so as to better illustrate its role. An order of magnitude calculation of the electrostatic torque is also provided, to show that the scales for these steering torques are comparable. Indeed, our models of cleft systems suggest that the hydrodynamic torque can be 2 orders of magnitude greater.

GOVERNING EQUATIONS

To assess the importance of forces involved in protein interactions, it is necessary to have a way to measure the effect. This is usually done by extracting a reaction rate constant from an ensemble of Brownian simulations (5). The protein and ligand are placed in an initial configuration some distance apart and are released to move in solution under the influence of Brownian, electrostatic, and viscous forces. The governing differential equation for the motion is

$$\boldsymbol{m}\cdot\frac{d^2\boldsymbol{x}}{dt^2}+\boldsymbol{\zeta}\cdot\frac{d\boldsymbol{x}}{dt}-\boldsymbol{F}(\boldsymbol{x})=\Gamma(t), \qquad [1]$$

where $\boldsymbol{m}$ are generalized masses, $\boldsymbol{x}$ are generalized coordinates of the particles, and $\boldsymbol{F}$ are generalized forces. In this paper these generalized forces are taken to be forces and torques in the coordinate directions. Here Γ is a stochastic "driving force" for the motion, and $\boldsymbol{\zeta}$ is the friction coefficient matrix relating the hydrodynamic forces and torques on the particles to their velocities. In the hydrodynamics literature, the solvent viscosity μ is usually scaled out of the friction coefficient matrix, so that all components have dimensions which are powers of length. The resulting matrix is called the resistance matrix.

The equation of motion can be integrated to obtain the evolution equation for the particle position:

$$\Delta\boldsymbol{x}=\nabla\cdot\boldsymbol{D}\Delta t+\frac{\boldsymbol{D}\cdot\boldsymbol{F}}{kT}\Delta t+\boldsymbol{X}(\Delta t); \qquad [2]$$

its derivation is detailed in ref. 6. In this equation, $\boldsymbol{D}$ is the "diffusion matrix" for the problem, the inverse of the friction coefficient matrix. As for the friction coefficient matrix, μ can be factored out, leaving what is called the mobility matrix. Values of $\boldsymbol{X}$ are selected from a gaussian distribution with mean zero and autocorrelation $2\boldsymbol{D}\Delta t$.

Once a sufficient number of simulations has been carried out, a reaction rate constant can be extracted from the fraction of particles which react (7–9).

In the evolution equation for two particles, the friction coefficient and diffusion matrices are 12 × 12, relating the translational and rotational velocities of each particle to the hydrodynamic forces and torques on each particle:

$$\begin{pmatrix}\boldsymbol{F}_{\mathrm{H}}^{(1)}\\ \boldsymbol{F}_{\mathrm{H}}^{(2)}\\ \boldsymbol{T}_{\mathrm{H}}^{(1)}\\ \boldsymbol{T}_{\mathrm{H}}^{(2)}\end{pmatrix}=-\mu\begin{pmatrix}\boldsymbol{A}^{(11)} & \boldsymbol{A}^{(12)} & \tilde{\boldsymbol{B}}^{(11)} & \tilde{\boldsymbol{B}}^{(12)}\\ \boldsymbol{A}^{(21)} & \boldsymbol{A}^{(22)} & \tilde{\boldsymbol{B}}^{(21)} & \tilde{\boldsymbol{B}}^{(22)}\\ \boldsymbol{B}^{(11)} & \boldsymbol{B}^{(12)} & \boldsymbol{C}^{(11)} & \boldsymbol{C}^{(12)}\\ \boldsymbol{B}^{(21)} & \boldsymbol{B}^{(22)} & \boldsymbol{C}^{(21)} & \boldsymbol{C}^{(22)}\end{pmatrix}\cdot\begin{pmatrix}\boldsymbol{U}^{(1)}\\ \boldsymbol{U}^{(2)}\\ \boldsymbol{\omega}^{(1)}\\ \boldsymbol{\omega}^{(2)}\end{pmatrix} \qquad [3]$$

and

$$-\mu\begin{pmatrix}\boldsymbol{U}^{(1)}\\ \boldsymbol{U}^{(2)}\\ \boldsymbol{\omega}^{(1)}\\ \boldsymbol{\omega}^{(2)}\end{pmatrix}=\begin{pmatrix}\boldsymbol{a}^{(11)} & \boldsymbol{a}^{(12)} & \tilde{\boldsymbol{b}}^{(11)} & \tilde{\boldsymbol{b}}^{(12)}\\ \boldsymbol{a}^{(21)} & \boldsymbol{a}^{(22)} & \tilde{\boldsymbol{b}}^{(21)} & \tilde{\boldsymbol{b}}^{(22)}\\ \boldsymbol{b}^{(11)} & \boldsymbol{b}^{(12)} & \boldsymbol{c}^{(11)} & \boldsymbol{c}^{(12)}\\ \boldsymbol{b}^{(21)} & \boldsymbol{b}^{(22)} & \boldsymbol{c}^{(21)} & \boldsymbol{c}^{(22)}\end{pmatrix}\cdot\begin{pmatrix}\boldsymbol{F}_{\mathrm{H}}^{(1)}\\ \boldsymbol{F}_{\mathrm{H}}^{(2)}\\ \boldsymbol{T}_{\mathrm{H}}^{(1)}\\ \boldsymbol{T}_{\mathrm{H}}^{(2)}\end{pmatrix}. \qquad [4]$$

In this representation, we have scaled μ out and divided the resulting matrices into the component tensors. Superscripts on the forces, torques, and velocities represent the particle in question. For each of the tensors, the first superscript represents the particle which is affected, and the second represents the particle which is causing the effect. Tensors $\boldsymbol{A}$ and $\boldsymbol{a}$ relate forces $\boldsymbol{F}_{\mathrm{H}}$ to translational velocities $\boldsymbol{U}$; tensors $\boldsymbol{C}$ and $\boldsymbol{c}$ relate torques $\boldsymbol{T}_{\mathrm{H}}$ to rotational velocities $\boldsymbol{\omega}$; and tensors $\boldsymbol{B}$ and $\boldsymbol{b}$ describe coupling effects. Of the 144 total tensor components, 78 are independent, since the matrices are symmetric (10). Since the matrices are configuration dependent, it is necessary to recompute them when the orientation of the particles changes significantly.

Because of the difficulties associated with solving the two-particle hydrodynamics problem, assumptions have always been made about the diffusion/mobility matrix. The simplest (and very common) assumptions are that

(*i*) no coupling occurs—that is, that all off-diagonal terms are zero;

(*ii*) the three on-diagonal terms in each of the nonzero tensors are equal, given by a scalar diffusion coefficient; and

(*iii*) the diffusion coefficient does not vary with the configuration of the particles.

This reduces the 78 configuration-dependent constants in the diffusion matrix to four configuration-independent constants, each of which can be obtained experimentally. All off-diagonal tensors in the diffusion matrix are zero, while the on-diagonal tensors have the form

$$D\begin{pmatrix}1 & 0 & 0\\ 0 & 1 & 0\\ 0 & 0 & 1\end{pmatrix}. \qquad [5]$$

Some authors have relaxed the second assumption, incorporating experimental data about the direction dependence of the diffusion coefficient. This leads to on-diagonal tensors of the form

$$\begin{pmatrix}D_{11} & 0 & 0\\ 0 & D_{22} & 0\\ 0 & 0 & D_{33}\end{pmatrix}, \qquad [6]$$

but again, all off-diagonal terms are assumed zero. Others have relaxed the third assumption, modeling the configurational variation of the diffusion tensors by using the Oseen or Rotne-Prager tensors (6). Because of the simple form of these hydrodynamic interaction tensors, all off-diagonal terms in the diffusion tensor are again zero.

In a recent paper (11), an enzyme–substrate system was modeled as a sphere (enzyme) and two rigidly connected spheres (substrate). Hydrodynamic interactions between the two rigidly connected spheres composing the substrate were approximated by Oseen tensors at the sphere centers, but hydrodynamic interactions between the enzyme and substrate were neglected.

Assuming that all off-diagonal components in the diffusion matrix are zero removes some potentially important physics from the problem. For example, as enzyme and substrate are pushed together, hydrodynamic interactions between features of the enzyme and substrate may act to orient the substrate with the enzyme. This particular interaction would be summarized in four components of the b tensors, which are generally assumed to be zero.

In this paper, the full diffusion matrix for a model system will be presented, and the spatial variation of some of the key components of the diffusion matrix will be detailed. In principle, we can perform Brownian dynamic simulations from which a reaction rate constant can be extracted, using, for example, the approach given in ref. 12 to model the enzyme geometry. Indeed, on the next generation of massively parallel computers, such simulations will be possible. The scope of the present paper is limited to a demonstration of the importance of the hydrodynamic steering torque, so a smaller computational problem that fits in the time scale of a desktop workstation is considered. The magnitude of the hydrodynamic torque will be estimated and compared to electrostatic torque to assess the importance of the hydrodynamic torque.

METHOD OF CALCULATION

To assess the impact of off-diagonal terms in the diffusion matrix, it was first necessary to find an appropriate model system. We chose the cleft enzymes (lysozyme, the serine proteases, and the kinases are examples). These enzymes can be viewed as globular, with a cleft cut out (Fig. 1), or alternatively, as two globular subdomains, with a space in between that corresponds to the cleft (Fig. 2). The substrate, generally long and thin, fits into the cleft. The model used, shown in Fig. 2, is an assembly of two spheres of diameter 40 Å, separated by a distance of 10 Å. This is the same geometry used in a previous study of the cleft enzyme lysozyme (13), although we use slightly larger dimensions, roughly consistent with the size of phosphoglycerate kinase. The substrate was modeled as a capsule, 40 Å long and 10 Å in diameter.

The cleft enzymes were chosen because they are fairly common, and they have a geometry that is likely to show

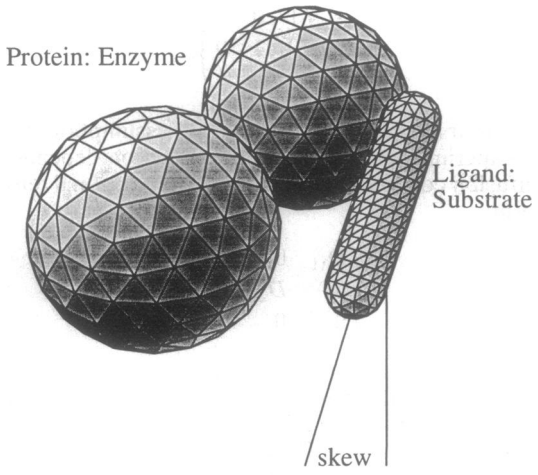

FIG. 2. Model system.

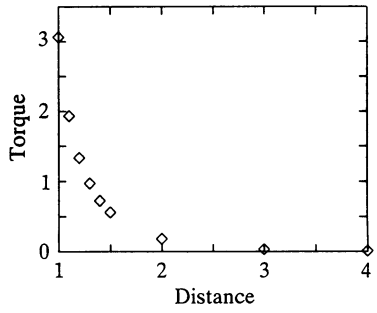

FIG. 3. Variation of steering torque with distance between substrate and enzyme cleft.

important coupling effects. Referring to the model figure, it is reasonable to expect that, as any external force moves the enzyme and substrate together, hydrodynamic interactions between the enzyme and substrate will act to orient the enzyme with the axis of the cleft.

Ordinarily, in calculating the diffusion matrix, one would solve the hydrodynamic mobility problem: that is, a unit force in a single coordinate direction would be applied to a single particle, and the velocities of all the particles would be obtained. These velocities correspond to elements in the first column of the diffusion matrix. By applying a series of different forces and torques, the diffusion matrix can be determined column by column. A very efficient iterative numerical method is available for solving the hydrodynamic mobility problem (10, 12).

In the model system (Fig. 2), there are three particles, two spheres and a capsule; the two spheres act as a single rigid body, the enzyme. Since it is not possible to specify *a priori* the combination of forces which will make the two spheres act as a single rigid body, an alternative approach was used, in which the velocities are specified and the forces are determined, the so-called "resistance problem."

Giving the two spheres a combination of velocities so that they behaved as a single rigid body "enzyme," we solved for the forces and torques on the rigid bodies, using the method of Power and Miranda (14). Standard Linpack routines were used to solve the linear system. The force on the two-sphere "enzyme" could then be obtained by adding the forces on the two spheres and the torque by summing the moments of the forces and the torques on the two spheres. This enabled solution for successive columns of the resistance matrix. Once the resistance matrix was obtained, it could be inverted to obtain the mobility and diffusion matrices.

To assess the magnitude of hydrodynamic effects in protein association, we compare an average hydrodynamic restoring torque (i.e., a torque which tends to orient the substrate correctly to the enzyme active site) to an electrostatic restoring torque. For the cleft enzymes, as stated earlier, a hydrodynamic restoring torque would be produced if a sub-

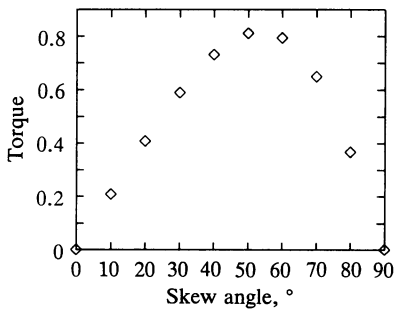

FIG. 4. Variation of steering torque with skew between substrate and enzyme cleft.

Table 1. Resistance matrix A tensors

31.4	0	−0.73	9.19	0	0.99
0	39.9	0	0	13.9	0
−0.73	0	32.5	0.82	0	6.83
9.19	0	0.82	12.8	0	1.18
0	13.9	0	0	16.4	0
0.99	0	6.83	1.18	0	10.7

strate and enzyme moved toward each other while the substrate and cleft axes were misaligned.

The magnitude of the restoring torque depends on two things: first, the magnitude of the coupling coefficients in the diffusion matrix, and second, the velocity in solution. The first has already been computed; the second must be estimated. Fortunately, this is not too difficult. To determine the strength of the Brownian forces on the particles, Eq. 1, the equation of motion for the particles, is manipulated to extract an average velocity for each degree of freedom of the system, in terms of the Brownian force strength. To satisfy equipartition of energy, the average velocity must satisfy

$$\frac{1}{2} m \left\langle \frac{dx}{dt} \right\rangle^2 = \frac{1}{2} kT, \qquad [7]$$

i.e., the kinetic energy for each degree of freedom must be $kT/2$. Once the strength of the Brownian forces is known, Eq. 1 can be integrated to obtain Eq. 2, the particle evolution equation, and simulated on a computer.

Since we are interested in average forces and torques, we do not need to carry out the simulations to obtain particle trajectories. The average velocity can be obtained as above, then used to directly calculate average forces and torques via the two-particle resistance matrix.

It must be kept in mind that the average velocity computed by using this method does not always push the enzyme and substrate together; it can just as easily move them apart, in which case the torque would tend to skew the substrate even further. The overall effect is that a substrate which moves *toward* an enzyme experiences a torque which *corrects* its misalignment, while a substrate which moves *away from* an enzyme becomes *even further misaligned*. This is of course exactly the kind of effect necessary to produce an increase in the number of substrate molecules that achieve the correct orientation to react.

For comparison purposes, we have calculated the restoring torque resulting from electric dipoles interacting in solution. Since we are interested in an order-of-magnitude comparison, we used a simple dipole model: equal and opposite charges separated by a distance chosen to roughly match the hydrodynamic model dimensions. Two sets of dipole interaction calculations were performed: one for a separation of 40 Å between the dipole charges and one for a separation distance of 5 Å. In each case, the magnitude of the charge was adjusted to produce a dipole moment of 300 debye (1 debye = 3.3×10^{-30} C·m) for each dipole, which Creighton (1) calls a large dipole moment. The interactions were treated as coulombic interactions with screening, using the Green function for the linearized Poisson–Boltzmann equation:

Table 2. Resistance matrix B tensors

−0.23	0	2.28	0.29	0	−3.74
0	1.00	0	0	0.89	0
7.32	0	1.48	9.74	0	1.65
−0.55	0	0.91	0.51	0	−0.31
0	1.08	0	0	−0.76	0
0.21	0	−0.47	0.38	0	0.19

Table 3. Resistance matrix C tensors

45.9	0	−0.12	−0.78	0	0.67
0	115.9	0	0	−3.06	0
−0.12	0	124.5	2.65	0	−2.74
−0.78	0	2.65	4.36	0	−2.52
0	−3.06	0	0	6.13	0
0.67	0	−2.74	−2.52	0	3.58

$$\phi(x) = \frac{\exp(-\kappa|x|)}{\varepsilon|x|}. \qquad [8]$$

The Debye length κ^{-1} was taken to be 7.5 Å, and a value of 80 was used for the dielectric constant ε. Both are typical values for physiological conditions.

RESULTS AND DISCUSSION

Variation of Hydrodynamic Interactions with Position. We chose a single distance (1.4 × the sphere radius of 20 Å) and varied the skew angle between 0° and 90°, then took a single skew angle (40°) and varied the distance separating the enzyme and substrate. The ordinate in both these plots is the steering torque on the substrate when the substrate approaches the (stationary) enzyme with unit velocity. It has been made dimensionless by scaling out the viscosity and radius of the enzyme spheres. Since the enzyme is much larger and less mobile than the substrate in solution, this is a good estimate for the steering torque in solution. Results are shown in graphical form in Figs. 3 and 4. As one would expect, the steering effect dies out with increasing separation distance and at skew angles of 0° and 90°.

Resistance/Mobility Tensors. For a separation of 1.4 × the sphere radius, and a skew angle of 40°, we have determined the full set of resistance/mobility tensors for the enzyme–substrate system. In these tensors, the "1" axis passes through the sphere centers, the "2" axis passes through the center of the substrate and the midpoint between the sphere centers, and the "3" axis is orthogonal to the other two. Tables 1, 2, and 3 show the A, B, and C portions of the resistance matrix, respectively. Only the symmetric portion was retained; the antisymmetric portion was very small, indicating that the hydrodynamic calculations were quite precise. Tables 4, 5, and 6 show the a, b, and c portions of the mobility matrix, respectively. The dimensions of all the matrix elements are powers of length. The elements have been scaled by the radius of the enzyme spheres to make them dimensionless.

Relative Magnitude of Hydrodynamic Steering Torque. To calculate a hydrodynamic steering torque, it is necessary to estimate the velocity of both the enzyme and the substrate. As stated earlier, the average thermal velocity necessary to give the molecules $kT/2$ of energy was used. This produces an average velocity of

Enzyme: 7.8 m/s.

Substrate: 37.5 m/s.

The Reynolds numbers for the enzyme and substrate place them well within the Stokes flow regime. Applying these average velocities to bring the substrate and enzyme closer together, together with the resistance tensors calculated in

Table 4. Mobility matrix a tensors (× 1000)

40.4	0	0.01	28.7	0	−0.52
0	35.6	0	0	30.1	0
0.01	0	35.7	0.02	0	22.6
28.7	0	0.02	104.0	0	7.69
0	30.1	0	0	86.6	0
−0.52	0	22.6	7.69	0	111.5

Table 5. Mobility matrix b tensors (× 1000)

0	0	−0.03	0.02	0	7.98
0	0	0	0	−0.26	0
0.12	0	−0.01	−6.23	0	0.50
3.46	0	−6.42	−3.08	0	2.82
0	−2.53	0	0	−5.33	0
3.23	0	−0.96	2.02	0	−1.12

the previous section, average torques on both enzyme and substrate can be computed at a separation distance of 28 Å and a skew angle of 40°:

Torque on the enzyme resulting from substrate motion toward the enzyme at the average substrate velocity: -1.34×10^{-19} N·m. The effect of this torque is to turn the enzyme so that its cleft is better aligned with the substrate.

Torque on the enzyme resulting from enzyme motion toward the substrate at the average enzyme velocity: -0.31×10^{-19} N·m. The effect of this torque is to turn the enzyme so that its cleft is better aligned with the substrate.

Torque on the substrate resulting from substrate motion toward the enzyme at the average substrate velocity: 1.14×10^{-19} N·m. The effect of this torque is to turn the substrate so that it is better aligned with the enzyme cleft.

Torque on the substrate resulting from enzyme motion toward the substrate at the average enzyme velocity: 0.36×10^{-19} N·m. The effect of this torque is to turn the substrate so that it is better aligned with the enzyme cleft.

Adding up the torques gives the following:

Total torque on the substrate resulting from enzyme and substrate approaching each other at their respective average velocities: 1.50×10^{-19} N·m.

Total torque on the enzyme resulting from enzyme and substrate approaching each other at their respective average velocities: -1.65×10^{-19} N·m.

The signs of these torques indicate that they both tend to better align the substrate with the enzyme cleft, one by acting on the substrate, the other by acting on the enzyme.

These torques can be compared to a torque from a large electrostatic dipole interaction, at the same distance of separation. For the "large" electrostatic dipole described earlier, the variation of the restoring torque with the skew angle between the dipole axes and the separation distance between dipole charges is shown in Table 7. The torque peaks at less than 10^{-21} N·m, more than 2 orders of magnitude *below* the average hydrodynamic steering torque. It is readily apparent that the hydrodynamic steering torque can be a very large quantity. Even allowing for errors in the approximate treatment of the electrostatics involved, and for the very simple hydrodynamic model used, it is clear that simulations which ignore hydrodynamic coupling effects for systems like the cleft enzymes will be ignoring a very large effect.

The comparison of hydrodynamic to electrostatic torque was made at a separation of 1.4 × the enzyme sphere radius, using a model which requires the adjacent fluid to stick to the enzyme and substrate. At this separation, using a zero tangential stress or "slip" model, as in ref. 15, would not materially affect the results. At separations much smaller than the local radius of curvature of the protein and ligand, however, there would be a substantial difference in the hydrodynamic forces predicted from using stick-and-slip models (10). Also, as the protein and ligand separation becomes small, it can be expected that hydrodynamic effects would become relatively less important, yielding to effects which have a stronger distance dependence, for example, dispersion or electrostatic forces. As a final caveat, it must be recognized that a substrate which is already misoriented from the enzyme cleft by greater than 90° will experience a further misorientation upon closer approach. The points above show the need for detailed simulations to quantify hydrodynamic effects on reaction rate.

There is no theoretical barrier to carrying out calculations for more realistic hydrodynamic models than are used here. However, more complicated models must be discretized more finely to obtain accurate results. This finer discretization leads to a larger set of equations and requires significantly more computer time for solution, making it even more difficult to carry out simulations with rigorously calculated hydrodynamic interactions. To carry out simulations, it will be necessary, at least for the immediate future, to use a method of calculating hydrodynamic interactions which is accurate enough to recognize coupling effects but simple enough to be evaluated during the course of a simulation. Singularity methods, for example (16), may be useful.

Table 6. Mobility matrix c tensors (× 1000)

22.5	0	0	3.28	0	−2.35
0	8.74	0	0	4.33	0
0	0	8.68	−1.79	0	4.69
3.28	0	−1.79	390.6	0	271.3
0	4.33	0	0	166.3	0
−2.35	0	4.69	271.3	0	474.2

Table 7. Electrostatic torque for interacting dipoles at charge separations of 40 and 5 Å

Skew angle, °	Torque, N·m × 10^{23} 40 Å	5 Å
0	0.0	0
10	4.9	10
20	8.5	19
30	10.2	28
40	10.1	36
50	9.1	42
60	7.8	48
70	6.6	52
80	5.8	54
90	5.6	55

This work was supported in part by a fellowship from the National Science Foundation and by grants from the Office of Naval Research and the National Science Foundation.

1. Creighton, T. E. (1984) *Proteins: Structures and Molecular Properties* (Freeman, New York).
2. Garcia de la Torre, J. & Bloomfield, V. A. (1981) *Q. Rev. Biophys.* **14**, 81–139.
3. Schurr, J. M. & Schmitz, K. S. (1976) *J. Phys. Chem.* **80**, 1934–1936.
4. Chou, K. C. & Zhou, G. P. (1982) *J. Am. Chem. Soc.* **104**, 1409–1413.
5. Allison, S. A. & McCammon, J. A. (1985) *J. Phys. Chem.* **89**, 1072–1074.
6. Ermak, D. L. & McCammon, J. A. (1978) *J. Chem. Phys.* **69**, 1352–1360.
7. Northrup, S., Allison, S. A. & McCammon, J. A. (1984) *J. Chem. Phys.* **80**, 1517–1524.
8. Luty, B. A., McCammon, J. A. & Zhou, H. X. (1992) *J. Chem. Phys.* **97**, 5682–5686.
9. Zhou, H. X. (1990) *J. Phys. Chem.* **94**, 8794–8800.
10. Kim, S. & Karrila, S. (1991) *Microhydrodynamics: Principles and Selected Applications* (Butterworth-Heinemann, Boston).
11. Luty, B. A., Wade, R. C., Madura, J. D., Davis, M. E., Briggs, J. M. & McCammon, J. A. (1993) *J. Phys. Chem.* **97**, 233–237.
12. Brune, D. A. & Kim, S. (1993) *Proc. Natl. Acad. Sci. USA* **90**, 3835–3839.
13. McCammon, J. A., Gelin, B. R., Karplus, M. & Wolynes, P. G. (1976) *Nature (London)* **262**, 325–326.
14. Power, H. & Miranda, G. (1987) *SIAM J. Appl. Math.* **47**, 689–698.
15. Wolynes, P. G. & McCammon, J. A. (1977) *Macromolecules* **10**, 86–87.
16. Dabros, T. (1985) *J. Fluid Mech.* **156**, 1–21.